High Resolution Current & Bathymetry Determined by Nautical X-Band Radar in Shallow Waters

Katrin Hessner[1] and Paul S. Bell[2]
[1] OceanWaveS GmbH, Lüneburg, Germany
[2] Proudman Oceanographic Laboratory, Liverpool, United Kingdom.

Abstract - **The wave and current monitoring system WaMoS II is a remote sensing system based on a nautical X-Band radar generally used for navigation and ship traffic control. It has been used in recent years to monitor sea state information from moored platforms, coastal sites and moving vessels. A nautical radar can scan the sea surface over a large area (~ 10km^2) with a high spatial (~7.5m) and temporal resolution (~2s). Directional wave spectra and standard sea state parameters such as significant wave height, peak wave period and direction can be derived by analyzing the sea surface image sequences. Using the temporal and spatial evolution of the sea surface wave images it is also possible to determine high resolution current and bathymetry information.**

In the paper a brief introduction into the measuring principle of WaMoS II is given and results of a high resolution current and bathymetric mapping technique for shallow water areas (<20m) are presented. For validation these results are compared with model data and in-situ measurements.

INTRODUCTION

The bathymetry of coastal areas is of great importance for off-shore activities, ship traffic and coastal protection. Coastal erosion and accretion as well as human activities can lead to rapidly changing bathymetry. Bathymetric surveys are time consuming and expensive, therefore a growing interest has been shown in remote sensing techniques to infer water depths over large areas in order to anticipate the need for and better target high resolution in-situ surveys.

In shallow seas the propagation of the waves is influenced by the local water depth and current field. First attempts to remotely obtain coastal bathymetry based on this effect were carried out using aerial photographs for military purposes [1]. Standard X-band nautical radar systems allow the monitoring of spatially varying wave fields with high temporal resolution under almost all weather conditions [2, 3] and so have the potential to be used for bathymetry retrieval in shallow seas [4, 5, 6, 7].

The data presented here were captured using the Wave Monitoring System WaMoS II, which is a high-speed video digitizing and storage device for nautical radars that delivers image sequences of the sea surface and sea state information based on those image sequences in near-real time.

STUDY AREA & GROUND TRUTH

The test site is located at the southern tip of the German Island of Sylt (Figure 1) – one of the islands enclosing the northern part of the Wadden Sea.
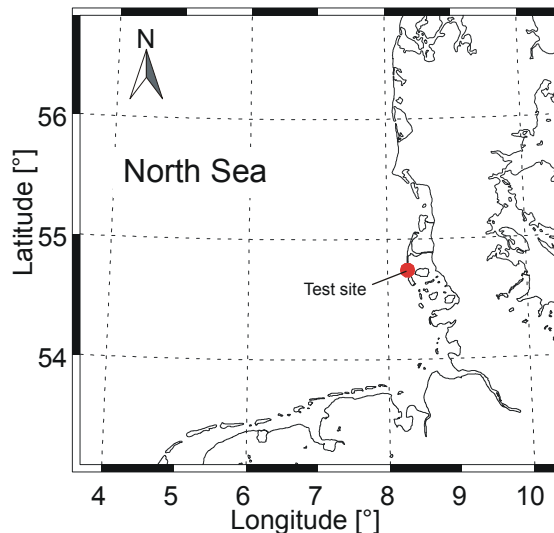

Figure 1. Map of the North Sea showing the location of the test site at the southern tip of the German Island Sylt.

The topography of the test site is characterized by extensive intertidal areas, sand banks and channels. The sediments are mainly sandy, and the sand banks and channels are extremely dynamic, varying constantly in size and position. The mean tidal range at Hörnum tide gauge station is about 2m, with tidal currents up to 1m/s. Prevailing wind and wave directions are W to NW and the mean wave height is of the order of 1m [8].

Fig. 2 shows a local map of the test site including the locations corresponding to the reference data. The blue crosses indicate the locations of grid points of the German Bundesamt für Seeschifffahrt und Hydrographie (BSH) circulation model. The current and water level comparison shown later is indicated by the yellow prism. The blue circle indicates the position of the wave buoy, and the green one the location of the tide gauge at Hörnum harbor. The red dot in the center of the radar image indicates the location of the radar antenna, which was mounted on a lighthouse approximately 40m above the sea level. The image of the radar backscatter intensity indicates the extent of the radar coverage with a recorded range of 450m – 1650m. On the seaward side of the island wave signatures of the eastward propagating wave are visible. In the southeastern corner signatures of submerged topographic features are visible. The white box indicate the standard WaMoS II analysis area for which the sea state and current comparison is shown.
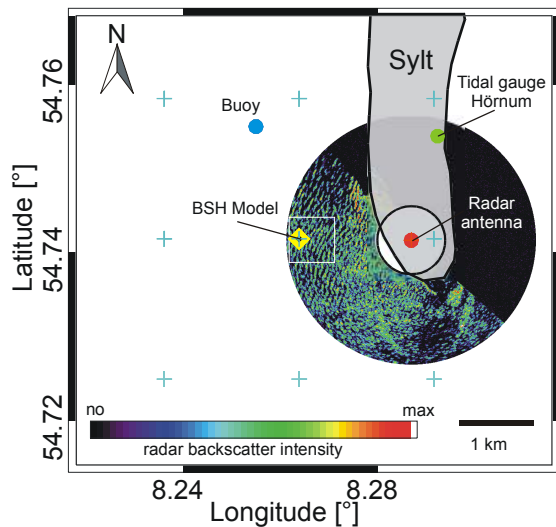
Figure 2. Map of the test site indicating the locations of the reference data. The radar image indicates the radar coverage of the WaMoS II system. The crosses indicate the BSH model grid points.

All relevant WaMoS II system parameters are summarized in Table 1.

TABLE I
WAMOS II SPECIFICATION

Parameter	Abbreviation	Value
Radar repetition rate	RPT	1.35s
Spatial (radial) resolution	dr	4.69m
Radar range	R	450m – 1650m

In the present study we focus on a storm event that took place on March 21-22, 2004. Figure 3 shows the time series of the main sea state parameters during this period as obtained by a wave rider buoy deployed temporarily by the German GKSS research center and by the WaMoS II standard analysis.
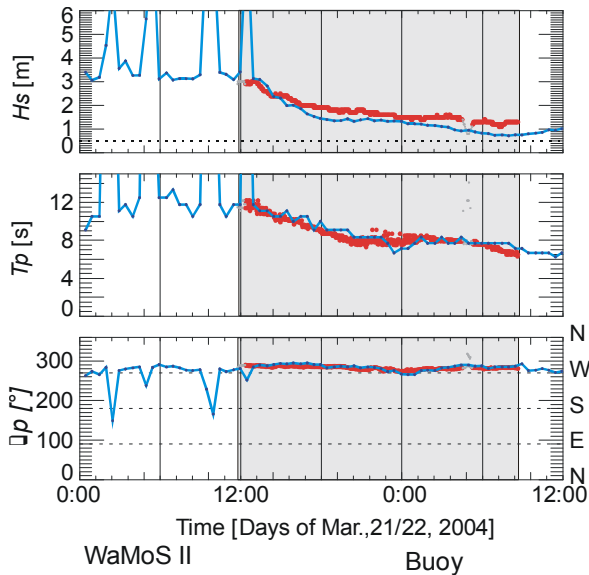

Figure 3. Time series of the mean sea state parameter significant wave height (Hs), peak wave period (Tp) and peak wave direction (θp, coming from) as obtained by the buoy (blue) and WaMoS II (red).

The grey areas indicate the times when raw radar data are available (March 21st, 11:45 – March 22nd, 08:39 UTC). During the peak of the storm on March 21st, 00:00-12:00 UTC heavy wave breaking took place in the test area and the wave buoy data show unrealistic spikes in the wave parameters (Hs > 3.5, Tp > 14s, θp < 200°). After the storm Hs decayed from around 3.5m to 1m and the wave periods from 12s to 6s. The waves approached the coast from WNW during the entire wave event. The buoy and WaMoS II derived sea state parameters show good agreement.

Survey Data

Two surveys were carried out by the Landesbetrieb für Küstenschutz National Park und Meeres Schutz (LKN) Germany., one recorded in 2002 and one in 2005 (Fig. 4). The track data have been gridded to 25m pixels. Despite the 2005 survey being closer in time to the wave event studied here, the arrangement of sandbanks and channels was more similar to the 2002 survey, and so only the 2002 survey is considered here. This striking difference in sand bank and channel locations between the two surveys emphasizes the dynamic nature of the bathymetry in this area.
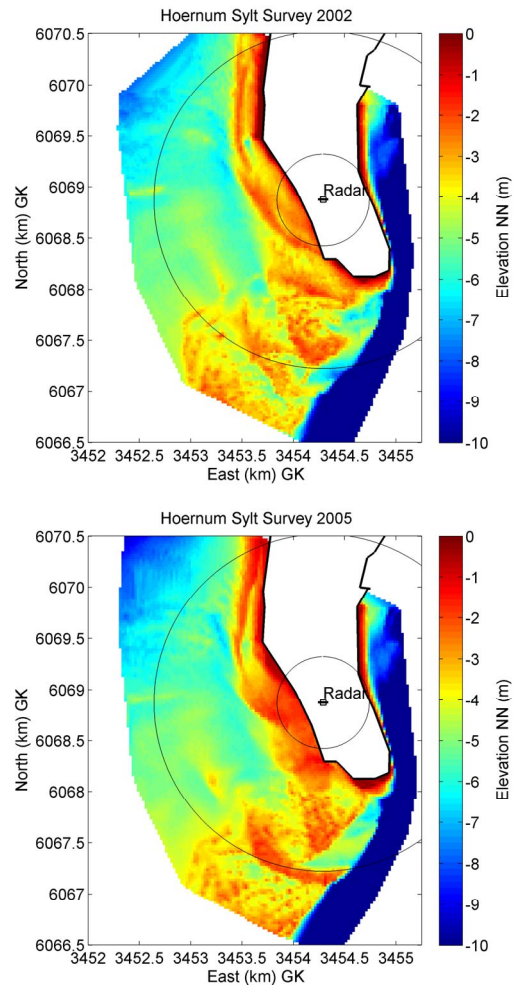

Figure 4. Survey data from 2002 and 2005 showing significant changes in the layout of sandbanks and channels around the southern tip of the island.

Model

The model data is an output of the 3-dimensional BSH circulation model [9] which takes into account meteorological forecasts for the North Sea and Baltic Sea provided by the German Weather Service (DWD), tides and external surges entering the North Sea from the Atlantic, as well as river runoff from the major rivers. To compute the heat fluxes between air and water, the BSH model uses wind and atmospheric pressure forecasts and additionally, measurements of air temperatures, clouds, and specific humidity above the sea. The tidal boundary values at the open model boundaries of the North Sea are computed from the harmonic constants of 14 tidal constituents. External surges entering the North Sea are computed using a model of the northeast Atlantic. In the circulation model, both the influence of wave action on the currents and water levels as well as density driven currents determined by current temperature and salinity distribution are taken into account.

The grid spacing is 1'40" in longitude ($\Delta x = 1784.50$m) and 1' in latitude ($\Delta y = 1855.40$m). The surface elevation is relative to NN. The results shown represent 15 minutes mean values in time and 3.2km^2 in space for the upper 5m layer of the model.

DATA ANALYSIS

Current Retrieval

The current measurement by WaMoS II is an indirect measurement, where the current is determined via the observation of the waves in time and space. As waves propagating in a current they experienced a frequency shift to higher frequencies while waves propagating against the current experience a shift to lower frequencies. This is the Doppler effect. Fig. 5 shows a schematic plot of a frequency (ω) - wave number (k) spectrum. Wave energy in the absence of surface currents is plotted in yellow and the corresponding wave energy Doppler shifted by a current is presented in blue. The surface current is quantified by determining the Doppler shift for each wave number.
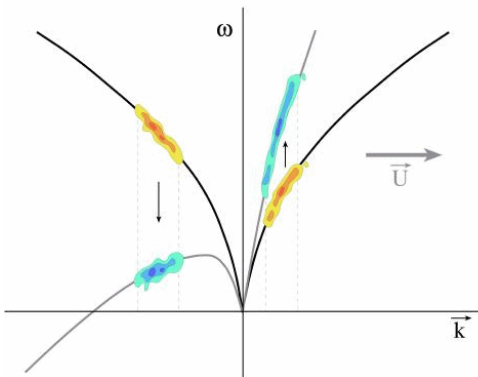

Figure 5. Schematic plot of the location of wave energy in a frequency - wave number spectrum in the absence of a current (yellow) and with current (blue).

Wave Parameter Data Comparison

Figure 6 shows time series plots of water depth with respect to NN (Normal Null), current speed and direction. The red dots indicate WaMoS II measurements representing 20 minutes mean updated every 1.5 minutes. The WaMoS II current was obtained for an area of 128x128 pixels (0.36km^2, see Figure 2). The green data refers to the corresponding BSH model data. Black indicates the surface elevation measured by the tide gauge at Hörnum Harbour.
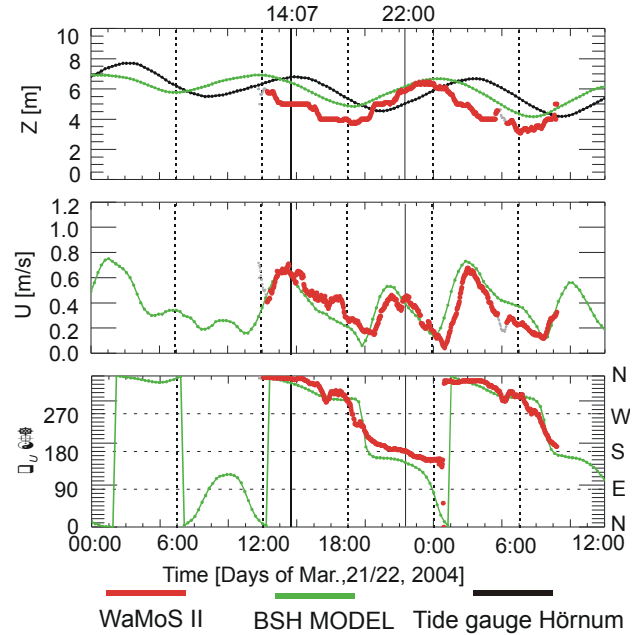

Figure 6. Time series of the water level (Z; upper panel), current speed (U, middle) and current direction (θ_U going to; lower panel).

The period shown spans 1.5 tidal cycles, during which the water level varied by about 2m. The mean water level for this model grid point is 5m. The maximum current occurred shortly after high water with maximum current speed of about 0.7m/s in northward direction. The ebb current with 0.55m/s is slightly weaker with southward direction. The time series generally show a good agreement between the model and the WaMoS II data. The WaMoS II data exhibit the general characteristic of the tidal elevation as well as the current, but with a noticeable phase shift in the water levels. High water in the radar analysis area occurs first, followed about half an hour later by the model grid point. This is to be expected as the model grid box extends to the south of the tip of the island and will be influenced by the flow through the inlet which will naturally have a phase lag while the lagoon fills. High water at the tide gauge is a further hour later despite its physical location being only a few kilometres away, due to its location well inside the lagoon.

High Resolution Currents & Bathymetry

The bathymetry and current maps were calculated using a similar process to that used by the standard WaMoS analysis, moving a 240m square analysis window at 60m intervals to

select the local 3D wavenumber spectrum. Then, rather than using linear wave theory that assumes perfectly sinusoidal waves, an engineering approximation to non-linear wave theory was fitted to the local wavenumber spectrum. This non-linear approximation includes a correction for the behaviour of waves of finite wave height [6, 10] and gives more accurate water depth estimates in shallow water. The solid vertical lines in Figure 6 indicate the times for which the water level and current fields derived by this method are shown in Figure 7 and Fig. 8 representing the northward flood and weaker southward ebb currents respectively. Only every other current vector has been plotted in these figures for clarity of presentation, although estimates exist for every pixel in the images.

Considerable variation of both current magnitude and direction can be seen in both plots, with particularly strong currents over the complex of sandbanks and channels to the south of the island, going some way to explaining the dynamic nature of the sandbank morphology in that area.
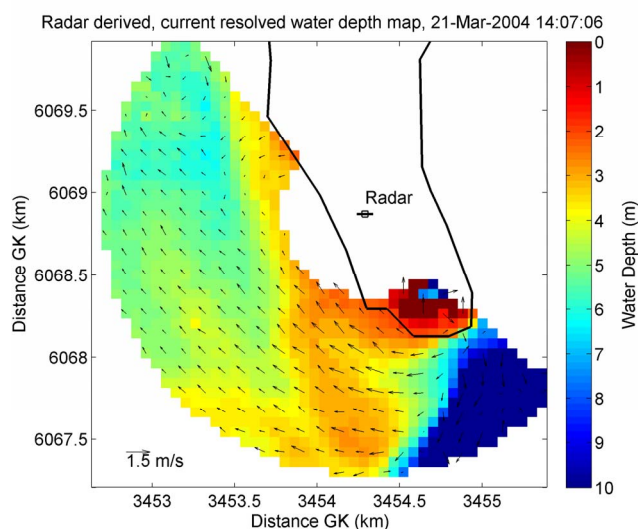
Radar derived, current resolved water depth map, 21-Mar-2004 14:07:06

Figure 7. Radar derived bathymetry and flood current field.

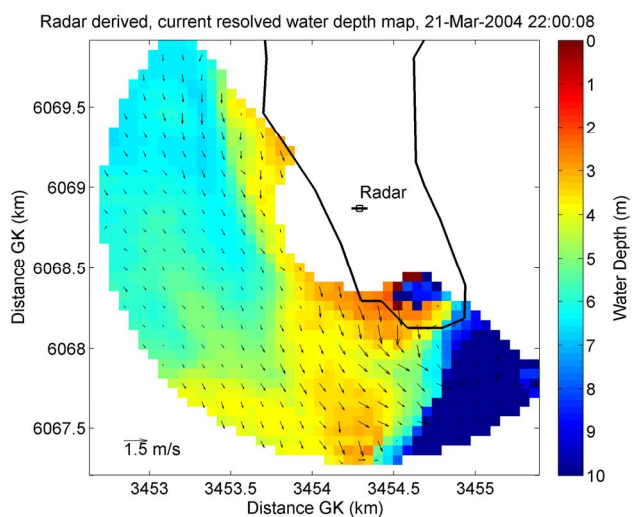Radar derived, current resolved water depth map, 21-Mar-2004 22:00:08

Figure 8. Radar derived bathymetry and ebb current field.

By subtracting the model water level from the radar derived water depth maps they can be corrected to the same datum used in the survey – Normal Null (NN), which approximates to mean sea level. This is a crude correction and takes no account of the significant tidal slope present in this relatively small area. For a more accurate tidal correction it would be necessary to use a very high resolution tidal model, which was beyond the scope of this paper.

Despite the crudeness of the tidal correction and the fact that the topography of the area at the time of the wave event shown here would not be well represented by either survey available to the authors, an attempt has been made to illustrate the scale of errors present in the bathymetry estimates.

The 2002 survey was considered the nearest approximation to the arrangement of sandbanks and channels at the time of the study, and this has been re-gridded to the pixel size of the radar derived output, i.e. 60m pixels (Fig. 9). This is obviously still a poor representation of the sandbanks to the south of the island, but is sufficient to demonstrate that the general form of the output is reasonable compared with the radar derived version shown relative to NN in Fig. 10. The difference between the two is shown in Fig. 11, demonstrating that large parts of the radar derived bathymetry are within 0.5m of the survey data, particularly in the more stable northern part of the study area. Few areas are more than 1m different from the survey and those are generally in the more dynamic parts of sandbanks where differences well in excess of 1m might be expected from year to year simply from the evolution of the sandbanks and channels and may well be genuine changes. An overall slight bias (blue shades in the plot) to the radar underestimating the wave depth may be an artifact of the crudeness of the tidal correction as this sort of bias has not been evident at other study sites. The difference in tidal phase illustrated in Fig. 6 suggests that it may be possible to identify the phase lag of the tide across the area from time series of radar derived water depths at different locations within the study area, hence allowing a more realistic correction to datum.

CONCLUSIONS

Analysis of nautical radar image sequences recorded using a WaMoS II system has demonstrated the ability to derive both wave and current parameters that compare well with buoy and model data. Further, a high resolution water depth and current mapping analysis has been demonstrated. Comparisons with survey data show that the radar derived bathymetric maps are generally within 1m of survey depths or better.

Although this study used data to a range of only 1.8km from the radar, other studies have shown that the same techniques are applicable to ranges of 4km and beyond under favorable wave conditions (Hs>1m). This technique could allow large areas of shifting sandbanks to be monitored remotely from the shore in order to better target high resolution in-situ surveys.
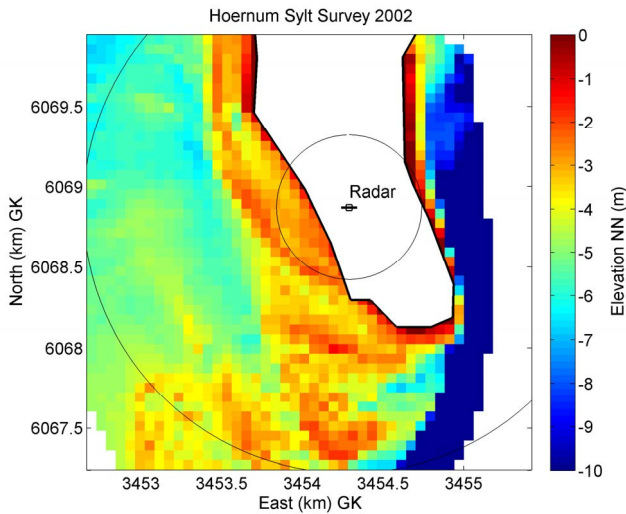
Figure 9. 2002 survey data gridded to the 60m pixel size of the radar output.
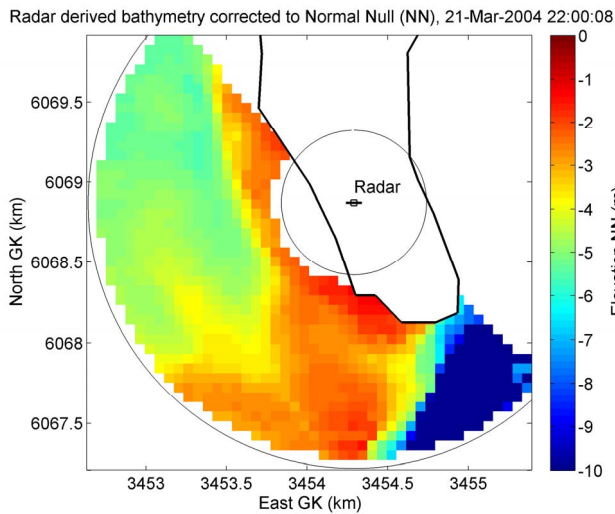

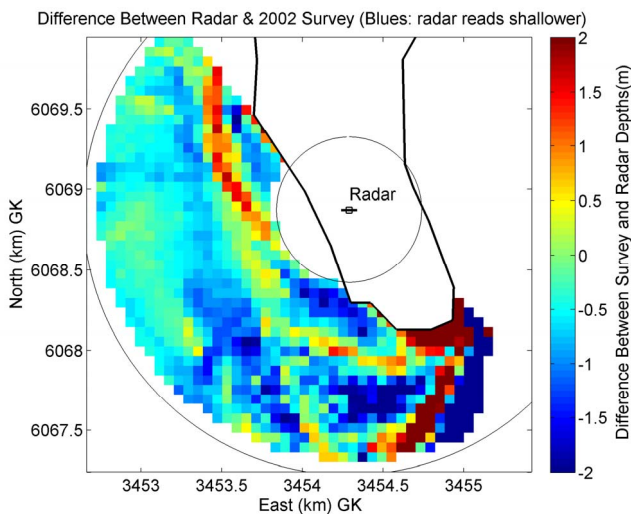Figure 10. Radar derived bathymetry with a tidal correction to NN.

Figure 11. The difference between the radar derived bathymetry and the 2002 survey data. Reds indicate that the radar is reading deeper than the survey, blues that the radar is indicating shallower than the survey.

REFERENCES

[1] Hart, C.A., and E.A. Miskin, "Developments in the method of determination of beach gradients by wave velocity," *Air survey research paper* No. 15, pp. 1-54, 1945.

[2] Young, I.R., Rosenthal W. and Ziemer F., "A Three-dimensional analysis of marine radar images for the determination of ocean wave directionality and surface currents". *J.Geophys.Res*., Vol. 90, pp. 1049 – 1059, 1985.

[3] Nieto, J.C., K. Reichert, and J. Dittmer, "Use of Nautical Radar as a Wave Monitoring Instrument," *Coastal Engineering, 37, 331-342*, 1999.

[4] Bell, P.S., "Shallow water bathymetry derived from an analysis of X-band marine radar images of waves," *Coastal Engineering* (37), 3-4, pp.513-527, 1999.

[5] Hessner, K., Reichert, K. and Rosenthal, W., "Mapping of sea bottom topography in shallow seas by using a nautical radar," *2nd Symposium on Operationalization of Remote Sensing*, ITC, Enschede, Netherlands, 16-20 August 1999.

[6] Bell, P.S., Williams, J.J., Clark, S., Morris, B.D. and Vila-Concejo, A., "Nested Radar Systems for Remote Coastal Observations." *Journal of Coastal Research, SI39 (Proceedings of the 8th International Coastal Symposium*, Itajaí, SC, Brazil, 14-19 March 2004): 483-487. 2006.

[7] Bell, P.S., "Mapping of bathymetry and tidal currents in the Dee Estuary using marine radar data." *Proceedings of PECS 2008: Physics of Estuaries and Coastal Seas*, 25–29 August 2008, Liverpool (UK), 175–178, 2008.

[8] Hofstede, J.L.A., "Process-response analysis for Hörnum tidal inlet in the German sector of the Wadden Sea", *Quaternary International*, 60, 107-117, 1999.

[9] http://www.bsh.de/en/Marine_data/Forecasts/Prediction_models/index.js

[10] Hedges, T.S., "Empirical modification to linear wave theory." *Proceedings of the Institution of Civil Engineers Part 2 - Research and Theory*, 61(SEP): 575-579, 1976.